Composition dependence of lithium diffusivity in lithium niobate at high temperature

D. H. Jundt and M. M. Fejer
Applied Physics Department, Stanford University, Stanford, California 94305

R. G. Norwood and P. F. Bordui
Crystal Technology Inc., 1051 East Meadow Circle, Palo Alto, California 94303

(Received 13 March 1992; accepted for publication 23 June 1992)

An investigation was performed on the diffusivity of lithium in lithium niobate at 1100 °C in the crystallographic z direction over the composition range from 48.38 to 49.85 mol % Li_2O. A vapor transport technique was applied to produce a lithium niobate crystal with a widely varying diffusion-limited lithium concentration profile. The profile was measured through spatially resolved measurement of the phase-match temperature for frequency doubling of a Nd:YAG laser. A Boltzmann–Matano analysis was applied to the profile to estimate diffusivity as a function of composition. The validity of the Boltzmann–Matano results was examined through numerical simulation, taking into account finite interfacial mass transport. A dramatic increase of lithium diffusivity with Li/Nb ratio was observed, ranging from roughly 3×10^{-9} cm^2/s at the 48.38 mol % Li_2O congruent composition to roughly 50×10^{-9} cm^2/s at 49.85 mol % Li_2O.

I. BACKGROUND AND INTRODUCTION

Lithium niobate is a single-crystal material extensively used in a variety of optical and acoustic devices. Although the phase exists over a wide solid solution range, from roughly 44 to 50 mol % Li_2O, almost all commercially produced lithium niobate substrate material has a composition near the congruently melting value of 48.38 mol % Li_2O.[1] A variety of post-growth processing techniques are applied to lithium niobate to produce crystals or regions of crystals having altered composition. Notable among these are techniques to manufacture optical waveguides[2,3] and lithium enrichment to produce entire crystals with altered optical properties.[4,5] Many of these post-growth processing operations involve as an important mechanism the diffusion of lithium through the lithium niobate crystal. Understanding, optimization, and control of these operations therefore requires an understanding of lithium diffusivity.

Present understanding of lithium diffusivity in lithium niobate is far from complete. Published estimates of lithium diffusivity at 1100 °C vary over two orders of magnitude.[2,6] Conflicting reports have been made[7,8] regarding the dependence of lithium diffusivity on Li/Nb ratio.

The purpose of the present work was to investigate the diffusivity of lithium in lithium niobate at high temperature and its dependence on Li/Nb ratio. We applied a vapor transport technique[5,9] to produce a crystal with a widely varying diffusion-limited lithium concentration profile. We measured that profile through spatially resolved measurement of the phase-match temperature for frequency doubling of a Nd:YAG laser. We then applied a Boltzmann–Matano analysis to the profile to estimate diffusivity as a function of composition. Finally, we examined the validity of the Boltzmann–Matano results through numerical simulation, taking into account finite interfacial mass transport.

II. EXPERIMENTAL PROCEDURE

A. Sample preparation

The use of a vapor transport technique to change the Li/Nb ratio of lithium niobate crystals has been previously reported.[5,9] In essence, the technique consists of annealing crystal samples in close proximity to a relatively much larger mass of lithium niobate powder of a desired composition. Given sufficient time at sufficiently high temperature, the Li/Nb ratio in the crystal changes so as to approach that in the powder via a mechanism involving vapor transport and solid-state diffusion. Previous reports[9] have indicated that the lithium diffusion step tends to dominate the overall process kinetics. As such, the technique may be reasonably applied to investigate the lithium diffusion process.

Starting crystals for vapor transport processing were fabricated from poled Czochralski-grown boules of congruent composition. Crystals were saw cut into x-, y-, and z-oriented plates, each roughly 14 mm^2 by 3 mm in thickness.

Lithium-rich two-phase powder charges were prepared using Li_2CO_3 and Nb_2O_5 as starting chemicals. Powder ratios were chosen to establish a net composition of 65 mol % Li_2O. The powders were mixed, reacted, milled, and then rereacted to ensure compositional homogeneity. The vapor processing itself was carried out as described in Ref. 9, with the lithium niobate crystals supported slightly above the surface of a mass of powder in turn contained in a platinum crucible. Processing temperature was 1100 ±0.5 °C, determined using a calibrated thermocouple inserted into the bulk of a powder charge. Dry oxygen was flowed through the furnace at a continuous rate of roughly 60 ℓ/h.

Vapor processing was carried out for 24 h. By way of reference, previous work[9] has indicated processing times in

 0021-8979/92/203468-06$04.00

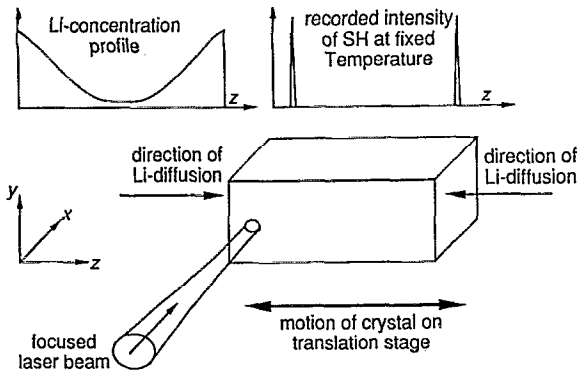

FIG. 1. Setup used to measure the phase-matching temperature as a function of depth beneath the surface.

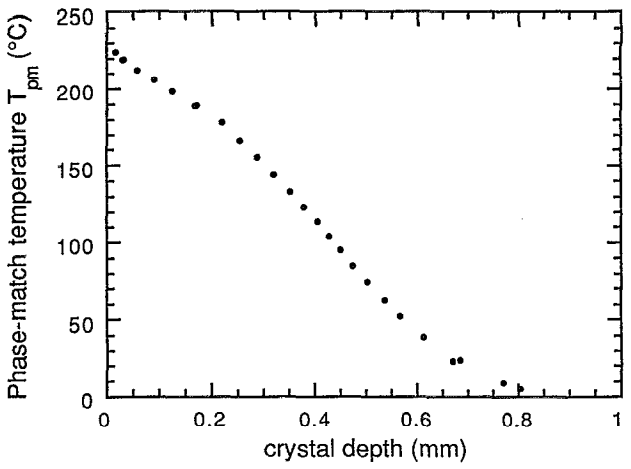

FIG. 2. Measured phase-matching temperatures for frequency doubling of a Nd:YAG laser as a function of depth.

excess of 600 h to be necessary to achieve compositional uniformity within 0.01 mol % Li_2O in such a system. Crucibles containing crystals and powder were removed from the 1100 °C furnace resulting in cooling to room temperature within 60 min.

In all cases, the processed x- and y-oriented plates were found to suffer extensive cracking severe enough to preclude further fabrication or testing, while the z-oriented plates were recovered intact. This was observed even when plates of different orientation were processed in the same crucible. It is notable that, in previous work,[9] both x- and y-oriented substrates were successfully recovered from vapor processing operations that were allowed to proceed much further toward an equilibrated state of compositional uniformity. This failure to recover intact plates of x and y orientation restricted the present work to the study of lithium diffusivity in the crystallographic z direction.

Each processed z-oriented crystal was prepared for measurement by saw cutting a rectangle roughly 1.5 mm in x by 2 mm in y from its central region. This was done to reduce any effects of diffusion in crystallographic directions other than z. The x-oriented end faces were polished to typical optical specifications.

B. Measurement of phase-matching temperature

The temperature for noncritically phase-matched laser frequency doubling T_{pm} is known to be a sensitive indicator of Li/Nb ratio in lithium niobate.[9,10] Figure 1 is a schematic of the method used in this work to measure T_{pm} for frequency doubling a 1.064 μm source. The laser beam was polarized along the crystallographic y axis and propagated along the x axis. The beam waist at the crystal was roughly 50 μm in diameter. The temperature of the oven was kept constant while the crystal sample was translated along its z axis and the intensity of the second harmonic recorded. The width of each of the two phase-matching peaks typically corresponded to 20 μm translation of the crystal. It is notable that, with this method, the propagation of the laser beam through the crystal depends solely on the ordinary index that changes only slightly with stoichiometry.[11] Beam bending is therefore absent and does not diminish the accuracy of the measurement in contrast to interferometric methods relying on measuring the extraordinary index. Scanning the crystal sample at a variety of constant temperatures and correcting for thermal expansion of the crystal yielded the data shown in Fig. 2 of T_{pm} versus depth in the crystal. These data were estimated to be accurate within ± 1 °C.

C. Correlation of Li/Nb ratio to phase-matching temperature

To correlate the measured T_{pm} values with Li/Nb compositional ratios, we used previously established data from 1.064 μm frequency doubling measurements performed on lithium niobate crystals equilibrated to a variety of controlled Li/Nb composition ratios using vapor processing techniques. Details of these measurements have been reported previously.[9] The phase-matching temperature of the samples increased smoothly with increasing composition except for the last data point very close to the lithium-rich phase boundary. A cubic polynomial fits the data well:

$$x = a + bT_{pm} + cT_{pm}^2 + dT_{pm}^3,$$

where

$$a = 48.35,$$
$$b = 8.7 \times 10^{-3}\ \mathrm{K}^{-1},$$
$$c = 3.1 \times 10^{-6}\ \mathrm{K}^{-2},$$
$$d = -4.7 \times 10^{-8}\ \mathrm{K}^{-3}, \quad (1)$$

with x in mol % Li_2O and T_{pm} in °C. The maximal discrepancy between Eq. (1) and the experimental data is 0.03 mol % Li_2O over the range from the 48.38 mol % Li_2O congruent composition to 50 mol % Li_2O.

Equation (1) was then applied to correlate Li/Nb composition ratio to the T_{pm} versus depth measurements from Fig. 2. Figure 3 shows the resulting curve of Li/Nb composition ratio versus depth. Solid lines show the orig-

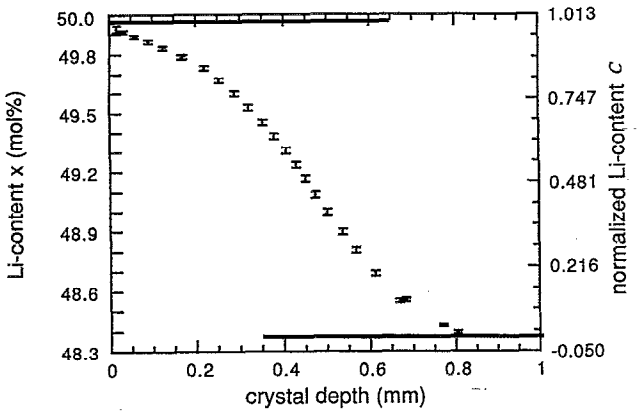

FIG. 3. Concentration vs depth for Li diffusion. The diffusion took place at 1100 °C for 24 h.

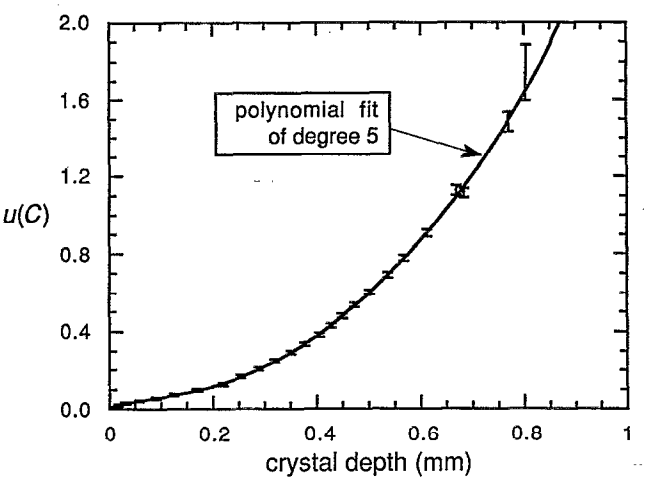

FIG. 4. Concentration vs depth with best fit after the variable transformation $u(z)=\mathrm{erfc}^{-1}[C(z)]$. The deviation from straight line behavior is indicative of a concentration-dependent diffusivity or finite interfacial mass transport.

inal congruent composition and an effective 1100 °C phase-boundary composition of 49.98 mol % Li_2O discussed below.

III. DATA ANALYSIS

A. Boltzmann–Matano method

It was convenient to express concentration by a normalized dimensionless variable C, which is zero for the starting material and one for the phase-boundary composition. Because of the previously reported[9] anomalous behavior of T_{pm} in the immediate vicinity of the Li-rich phase boundary, a convenient point on the curve of Eq. (1) was selected to represent the phase boundary. We chose the point 49.98 mol % Li_2O at 238 °C, keeping in mind that the resulting derived diffusivity values would be uncertain for compositions exceeding roughly 49.90 mol % Li_2O. The transformation between x and C was then given by

$$C=\frac{(x-x_{\text{initial}})}{(x_{\text{final}}-x_{\text{initial}})}=\frac{(x-48.38\%)}{1.6\%},$$

or correspondingly,

$$x=48.38\%+C\times 1.6\%. \tag{2}$$

To analyze the data, we assumed that the diffusion process could be described by the nonlinear diffusion equation

$$\frac{\partial C}{\partial t}=\frac{\partial}{\partial z}\left(D(C)\frac{\partial C}{\partial z}\right), \tag{3}$$

where $D(C)$ is the concentration-dependent Li-diffusion coefficient and z is the depth into the crystal plate. The initial condition at $t=0$ for the diffusion is $C=0$ throughout the volume.

Using a Boltzmann substitution to reduce the dimensionality of the problem, the diffusion coefficient could be calculated from the concentration versus depth profile using the technique developed by Matano,[12]

$$D(C)=-2\left(\frac{\partial C}{\partial \eta}\right)^{-1}\int_0^C d c'\eta,$$

where

$$\eta\equiv\frac{z}{2\sqrt{t}}. \tag{4}$$

The derivative involved in the Boltzmann–Matano method amplifies noise in the experimental data, so it is useful to smooth the data before evaluating Eq. (4). This smoothing is facilitated by first transforming the data points C_i according to $u_i=\mathrm{erfc}^{-1}(C_i)$, where erfc^{-1} is the inverse of the complementary error function. In this representation, a diffusion profile resulting from a concentration-independent diffusivity is a straight line. A polynomial of degree five was then fit to the u_i, shown in Fig. 4, and the smoothed diffusion profile was then obtained by the inverse transformation $C(z)=\mathrm{erfc}[u(z)]$ where $u(z)$ is given by the fitted polynomial. The diffusivity calculated according to Eq. (4) is shown in Fig. 5. It increases with increasing Li content, and varies by more than an order of magnitude over the compositional range investigated.

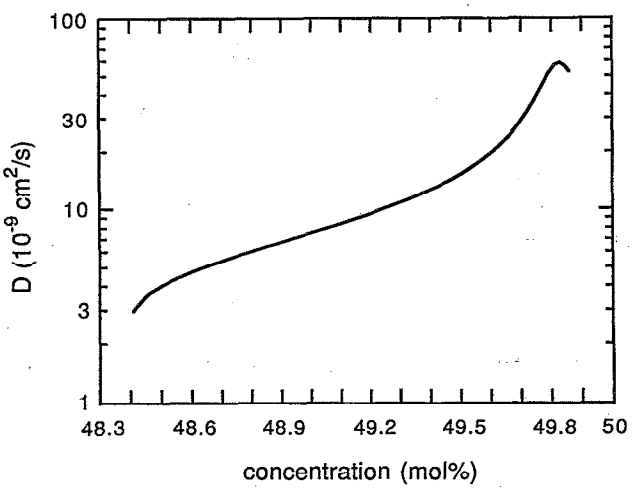

FIG. 5. Diffusivity resulting from a Matano analysis performed on the smoothed concentration vs depth data.

B. Validation of results through numerical simulation

The Boltzmann–Matano analysis is based on the Boltzmann substitution, which is only valid if the boundary condition can be expressed for all times by the same variable η defined in Eq. (4). In the case considered here, this requires that the concentration at the crystal surface be fixed at the value $C=1$ during the diffusion process.[13] To satisfy this condition, the initial flux of lithium through the surface has to be very high. The actual flux in the experiment might be limited to some lower value, diminishing the validity of the results from the Boltzmann–Matano technique. Diffusion fluxes have been estimated for out-diffusion processes and found to be in the range of 0.2–50 $\times 10^{-9}$ g/(cm^2 s).[3,5] Even though the surface flux for in-diffusion in a Li-rich atmosphere might be higher than that for out-diffusion, the finite value of the surface flux results in a surface concentration that deviates considerably from $C=1$ at short times. For long times, the crystal surface composition approaches the equilibrium composition, and the assumption underlying the Boltzmann substitution is approached.

To investigate the effect of a finite surface flux on the diffusion profile, the diffusion process was modeled numerically. The simplest boundary condition taking the kinetics at the surface into account has been proposed by Holman.[5] The vapor pressure of lithium niobate is assumed to be linearly dependent on the crystal composition. The flux through the surface is given by the difference in evaporation and condensation flux, where the evaporation flux is proportional to the composition of the crystal surface, and the condensation flux is determined by the vapor pressure of the phase-boundary composition. The net flux j through the surface is given by

$$j=\alpha(1-C)|_{z=0}=-D(C)\left.\frac{\partial C}{\partial z}\right|_{z=0}, \tag{5}$$

where α is the surface mass transfer coefficient depending on the vapor pressure of the phase-boundary composition. Equation (5) leads to a flux and composition at the crystal surface that both vary in time, and the Boltzmann substitution is no longer applicable. The boundary condition needed for a valid Boltzmann substitution is approached as a limiting case for $\alpha\rightarrow\infty$.

We investigated the effect of a finite value of α by numerically simulating the diffusion process with an algorithm using a forward projection of the diffusion coefficient to solve Eqs. (3) and (5),[14] The Li-concentration values were calculated for crystal depths spaced by 30 μm and time steps of 0.5 min. The value of the surface mass transfer coefficient was held constant while the concentration dependence of the diffusivity $D(C)$ was adjusted using a nonlinear least-squares routine (Levenberg–Marquardt method[15]) to yield the best agreement between the simulation and the measured data. The criterion for optimization is the chi-square parameter defined as

$$\chi^2=\sum_{\text{data point } i}\left(\frac{C_i-C_i^{\text{model}}}{\sigma_i}\right)^2, \tag{6}$$

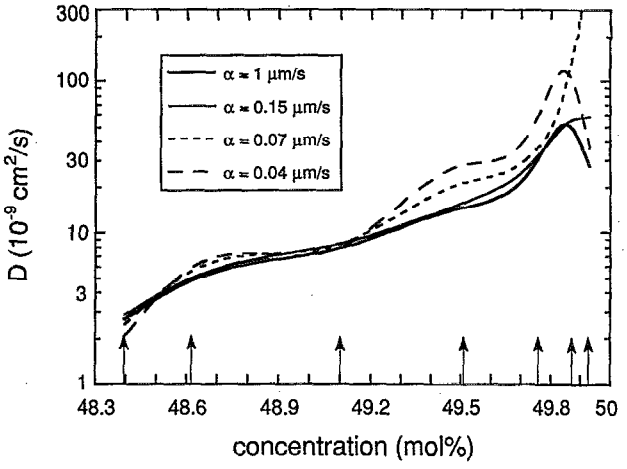

FIG. 6. Optimized diffusivity curves for different surface mass transfer coefficients. The seven adjustable parameters are the diffusivities at the concentrations denoted by arrows, and the values in between are interpolated with a cubic spline.

where C_i is the normalized concentration of the ith data point, σ_i its experimental uncertainty, and C_i^{model} the calculated concentration for the same depth and time as the data point. For the numerical simulation, the function $D(C)$ needs to be defined with the smallest number of freely adjustable fit parameters that can describe the true $D(C)$ dependence with sufficient accuracy. One parameter would only allow for a concentration independent diffusivity. To allow for such complicated curves as the one depicted in Fig. 5, seven adjustable parameters were used. The fit parameters correspond to the values of $\log(D)$ at the concentration values indicated with arrows in Fig. 6. The diffusivities for concentrations between these "anchor points" were calculated by a cubic spline interpolation[15] on $\log(D)$. The location of the anchor points was chosen such that the functional form shown in Fig. 5 was well approximated.

The optimized functional dependences of the diffusivity D on concentration for four different values of the surface mass transfer coefficient α are shown in Fig. 6. For the largest value of α shown, the function $D(x)$ closely resembles the result of Fig. 5, as expected. As the assumed surface transfer coefficient α of the simulation is decreased, the model compensates by increasing the diffusivity values in the range 49.1–49.8 mol % and decreasing them for the initial concentration. The calculated values for concentrations above 49.85 mol % do not follow a particular trend; the resultant diffusion profile is insensitive to the value of the highest anchor point. To estimate which of the values of α comes closest to the true value realized in the experiment, the residuals as defined in Eq. (6) are shown as a function of the assumed value of α in Fig. 7. The agreement between the experimental data and the simulation is excellent for α values larger than about 0.15 μm/s. The value of χ^2 in this range is around 6, indicating that the calculated concentration versus depth values lie well within the error bounds of the measured data points. As the assumed surface mass transfer coefficient is decreased

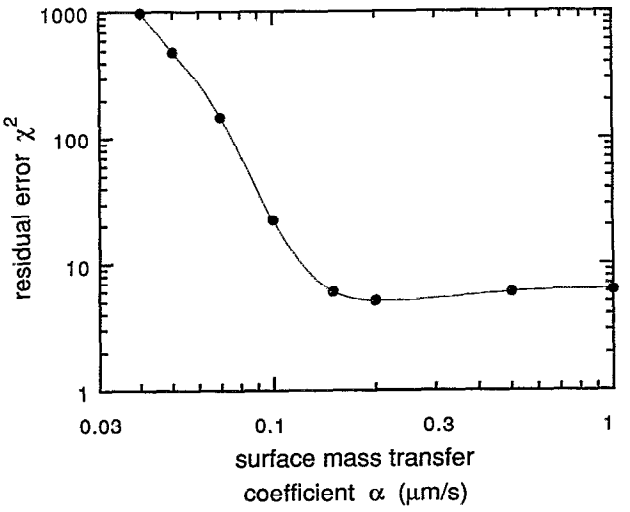

FIG. 7. Residual errors χ^2 as a function of the assumed surface mass transfer coefficient for optimized $D(C)$.

below 0.15 μm/s, the agreement degrades rapidly and a change in the diffusivity can no longer compensate for the low surface diffusion. Figure 8 compares the experimental data with the concentration profiles resulting from a numerical diffusion simulation with three different values of α. It is clear from Fig. 8 that the large residual errors for small α values stem from a surface concentration that is too low yield the observed result. The experimental data can only be explained adequately with a surface mass transfer coefficient that exceeds 0.1 μm/s.

Having established a lower limit of the surface mass transfer coefficient of $\alpha \approx 0.1$ μm/s, the implications on the validity of the Boltzmann substitution can be determined. The curves in Fig. 6 with α values 0.04 and 0.07 μm/s can be eliminated because they fail to yield a high enough surface concentration after a 24 h diffusion. The remaining two curves that give good agreement with the experimental data coincide for the composition range 48.4 to 49.5 mol %. They differ significantly for compositions larger

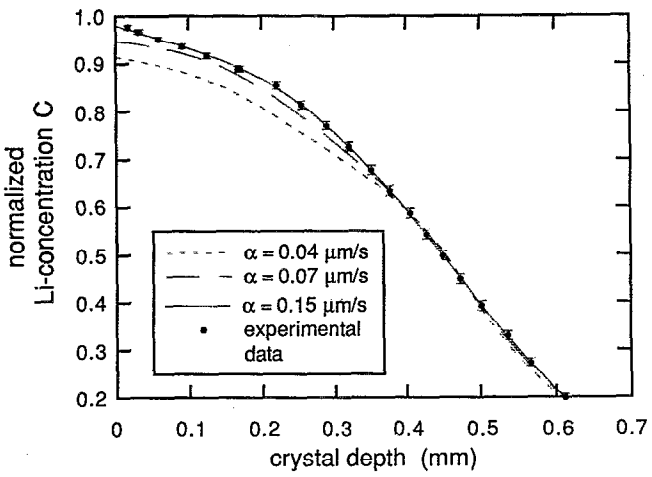

FIG. 8. Resulting concentration profiles for a 24 h diffusion with optimized $D(C)$ for different surface mass transfer coefficients.

than 49.85 mol %, suggesting that the experimental data are not adequate to determine the value of the Li diffusivity in that composition range.

It can thus be concluded that, as shown by the curves in Fig. 6 corresponding to the highest mass transfer coefficients, for the composition range 48.38–49.85 mol % Li_2O, the value of the lithium diffusivity in the crystallographic z direction at 1100 °C steadily increases from a value of 3×10^{-9} cm^2/s at the congruent composition to a value of 50×10^{-9} cm^2/s at 49.85 mol %. Considering all sources of error, these data can be considered accurate within $\pm 30\%$.

IV. DISCUSSION

The lithium diffusivity in lithium niobate as just presented is a chemical diffusivity. The experiment involved diffusion in a concentration gradient and therefore necessarily included associated niobium and oxygen diffusion effects. Accurate measurement of the composition dependence of the lithium self diffusivity in lithium niobate would require a series of experiments analyzing the transport of radioactive lithium tracer ions through a series of lithium niobate samples each having a different spatially constant Li/Nb ratio. It is notable, however, that many lithium niobate processing operations of interest actually involve a similar chemical diffusion process, occurring in the presence of a similar concentration gradient.

Although this is the first explicit report of the variation of lithium diffusivity with Li/Nb ratio, previous work[9] noted a dramatic increase observed in vapor transport processing time required to equilibrate lithium niobate crystals to powder charges of decreasing Li/Nb ratio.

To date, published discussions of the mechanisms for lithium diffusivity in lithium niobate at high temperature have generally assumed a vacancy process on the lithium sublattice to be dominant (see Ref. 16 and Refs. therein). Further, the high-temperature defect chemistry of lithium niobate has generally been assumed to involve a decrease in the lithium sublattice vacancy concentration with increasing Li/Nb ratio.[16] The observed increase in lithium diffusivity with increasing Li/Nb ratio thus suggests that transport of some other species is the rate limiting factor in the present process.

V. SUMMARY

An investigation was performed of the diffusivity of lithium in lithium niobate at 1100 °C in the crystallographic z direction over the composition range from 48.38 to 49.85 mol % Li_2O. A vapor transport technique was applied to produce a crystal with a widely varying diffusion-limited lithium concentration profile. That profile was measured through spatially resolved measurement of the phase-match temperature for frequency doubling of a Nd:YAG laser. A Boltzmann–Matano analysis was then applied to the profile to estimate diffusivity as a function of composition. Finally, the validity of the Boltzmann–Matano results was examined through numerical simulation, taking into account finite interfacial mass transport.

A dramatic increase of lithium diffusivity with Li/Nb ratio was observed, ranging from roughly 3×10^{-9} cm^2/s at the 48.38 mol % Li_2O congruent composition to roughly 50 $\times10^{-9}$ cm^2/s at 49.85 mol % Li_2O. The observed increase in lithium diffusivity with Li/Nb ratio suggests that lithium diffusivity is itself rate limited by transport of some other species.

ACKNOWLEDGMENTS

We thank Professor D. P. Birnie of the University of Arizona for numerous helpful discussions. D. H. Jundt and M. M. Fejer acknowledge the support by the Army Research Office under contract DAAL03-89-K-0113.

[1] P. F. Bordui, R. G. Norwood, C. D. Bird, and G. D. Calvert, J. Cryst. Growth **113**, 61 (1991).
[2] V. E. Wood, N. F. Hartman, A. E. Austin, and C. M. Verber, J. Appl. Phys. **52**, 1118 (1981).
[3] J. R. Carruthers, I. P. Kaminow, and L. W. Stulz, Appl. Opt. **13**, 2333 (1974).
[4] R. L. Holman, P. J. Cressman, and J. F. Revelli, Appl. Phys. Lett. **32**, 280 (1978).
[5] R. L. Holman, in *Processing of Crystalline Ceramics*, edited by H. Palmour and R. F. Davis (Plenum, New York, 1978), p. 343.
[6] V. B. Ptashnik, T. Y. Dunaeva, and I. V. Myasnikov, Izv. Akad. Nauk SSSR, Neorg. Mater. **21**, 2076 (1985).
[7] P. J. Jorgensen and R. W. Bartlett, J. Phys. Chem. Solids **30**, 2639 (1969).
[8] D. M. Smyth, Ferroelectrics **50**, 93 (1983).
[9] P. F. Bordui, R. G. Norwood, D. H. Jundt, and M. M. Fejer, J. Appl. Phys. **71**, 875 (1992).
[10] H. Fay, W. J. Alford, and H. M. Dess, Appl. Phys. Lett. **12**, 89 (1968).
[11] D. H. Jundt, M. M. Fejer, and R. L. Byer, IEEE J. Quantum Electron. **26**, 135 (1990).
[12] C. Matano, Jpn. J. Phys. **8**, 109 (1933).
[13] H. S. Carslaw and J. C. Jaeger, *Conduction of Heat in Solids*, 2nd ed. (Oxford University Press, London, 1959), pp. 89–91.
[14] D. U. von Rosenberg, *Methods for the Numerical Solution of Partial Differential Equations* (American Elsevier, New York, 1969), pp. 56–64.
[15] W. H. Press, B. P. Flannery, S. A. Teukolsky, and W. T. Vettering, *Numerical Recipes* (Cambridge University Press, Cambridge, 1986).
[16] D. P. Birnie, J. Mater. Sci. (in press).